Exact Coherent States of a Harmonically Confined Tonks-Girardeau Gas

A. Minguzzi and D. M. Gangardt

Laboratoire de Physique Théorique et Modèles Statistiques, Université Paris-Sud, Bât. 100, F-91405 Orsay, France*

(Received 8 April 2005; published 22 June 2005)

Using a scaling transformation we exactly determine the dynamics of an harmonically confined Tonks-Girardeau gas under arbitrary time variations of the trap frequency. We show how during a one-dimensional expansion a ''dynamical fermionization'' occurs as the momentum distribution rapidly approaches an ideal Fermi gas distribution, and that under a sudden change of the trap frequency the gas undergoes undamped breathing oscillations displaying alternating bosonic and fermionic character in momentum space. The absence of damping in the oscillations is a peculiarity of the truly Tonks regime.

DOI: 10.1103/PhysRevLett.94.240404 PACS numbers: 05.30.Jp, 03.65.Db, 03.75.−b

One of the most challenging and interesting problems in quantum dynamics involves understanding a temporal behavior of strongly correlated many-body systems beyond the linear-response regime or the adiabatic approximation. Aside from fundamental interest, this issue is of primary importance for current experiments with ultracold atomic gases and their potential applications to quantum information, where control and manipulation of entangled states of many-particle quantum systems is required.

The one-dimensional (1D) gas of impenetrable bosons (Tonks-Girardeau gas) corresponds to the limit of infinitely strong repulsive interactions in the Lieb-Liniger (LL) model of 1D bosons interacting through a contact pair potential [1]. It was shown in Ref. [2] that the Tonks-Girardeau limit is applicable for describing the low-density regime of bosonic atomic gases in a quasi-1D geometry. The physical properties of 1D bosons in this limit can be investigated in detail since their wave function is known explicitly in terms of the one of a noninteracting fermions in the same external potential [3]. In fact, the density profile, the thermodynamic properties, the collective excitation spectrum, and the density correlation functions coincide with those of an ideal Fermi gas, leading to interesting manifestations of fermionization of a Bose gas, such as broadening of the density profiles [4], an increase of the frequency of collective excitations [5] and a dramatic reduction of the three-body recombination rate [6]. However the one-body density matrix, and consequently the momentum distribution, differs considerably from that of a Fermi gas, due to the phase correlations stemming from the bosonic statistics of the Tonks gas. For the homogeneous case the momentum distribution $n(p)$ at the origin has a $1/\sqrt{p}$ peak [7] and for a harmonically trapped gas the population of the lowest single-particle state scales as $\sqrt{N}$ with N being the particle number [8,9]; this shows that due to the strong interactions the bosons do not form a Bose-Einstein condensate. In both cases at large momenta $p > \hbar n$, with n being the density at the center, the momentum distribution shows characteristic slowly decaying tails $n(p) \sim p^{-4}$ [10].

Experiments on cold atomic gases under optical confinement in a quasi-1D geometry are now starting to explore the strongly interacting regime, demonstrated by the examination of its correlation properties [11] and of the frequency of collective modes [12]. More recently there has been significant progress towards the Tonks limit, in which the momentum distribution [13] and the thermodynamical properties [14] have been measured. Experiments addressing the dynamics of the Tonks gas seem also in view. Some aspects of the dynamical evolution of a Tonks gas have already been theoretically studied. These include the formation of solitons in a ring geometry [15], the splitting and recombination of a Tonks beam across an obstacle [16] and 1D expansion [17]. In the last case, using numerical calculations on a lattice, the momentum distribution was found to approach that of an ideal Fermi gas [18].

The aim of this work is to study the dynamical evolution of a harmonically trapped Tonks gas induced by arbitrary time variations of the trap frequency. We show that this evolution can be described exactly using time-dependent coherent states (see, e.g., [19]), in close analogy of the dynamics of Bose-Einstein condensates [20]. These have been investigated also for the case of a strongly correlated Bose gas interacting with an inverse-square pair potential [21]. Here we explore, in particular, how the bosonic or fermionic properties of the Tonks gas manifest themselves in the dynamics of the coherence. For this purpose we choose the momentum distribution as the observable. We first determine explicitly its time evolution in terms of the initial-time configuration with the aid of a scaling transformation. We then use this result to study two important examples: (i) the 1D expansion of the gas, where we explain why the gas develops a Fermi shape of the momentum distribution, and (ii) the large-amplitude breathing modes, where we find the absence of damping and a rich dynamical evolution in momentum space, displaying alternating bosonic and fermionic character.

Scaling transformation.—We consider N impenetrable bosons with mass m in a 1D geometry at zero temperature and subjected to a harmonic potential

$$V_{\rm ext}(x,t) = m\omega^2(t)x^2/2 \quad (1)$$

with $\omega(t)$ arbitrary time-dependent trapping frequency and $\omega(t \leq 0) = \omega_0$. We proceed to derive an exact analytic expression for the evolution of the Tonks gas wave function, the one-body density matrix, and the momentum distribution at all times. We start by employing the time-dependent Bose-Fermi mapping [15], which allows us to write the many-body wave function $\Phi_T(x_1, x_2, \ldots, x_N; t)$ for the Tonks gas in terms of the wave function $\Phi_F(x_1, x_2, \ldots, x_N; t) = (1/\sqrt{N!}) \det_{j,k=1}^N \phi_j(x_k, t)$ of a noninteracting Fermi gas experiencing the same external potential. The single-particle orbitals $\phi_j(x,t)$ satisfy the time-dependent Schrödinger equation

$$i\hbar\frac{\partial}{\partial t}\phi_j(x,t) = -\frac{\hbar^2}{2m}\frac{\partial^2}{\partial x^2}\phi_j(x,t) + V_{\rm ext}(x,t)\phi_j(x,t). \quad (2)$$

The Tonks gas wave function is then constructed by applying to Φ_F the unit antisymmetric function $\mathcal{A}(x_1, \ldots, x_N) = \Pi_{1\leq j<k\leq N}\mathrm{sgn}(x_j - x_k)$,

$$\Phi_T(x_1, \ldots, x_N; t) = \mathcal{A}(x_1, \ldots, x_N)\Phi_F(x_1, \ldots, x_N; t), \quad (3)$$

and is thus properly symmetrized.

For the case of a time-dependent potential (1) the introduction of a scaling transformation for both the space and time coordinates provides an exact solution for Eq. (2), which reads [19,20]

$$\phi_j(x,t) = \frac{1}{\sqrt{b}}\phi_j\left(\frac{x}{b}, 0\right)\exp\left[i\frac{mx^2}{2\hbar}\frac{\dot{b}}{b} - iE_j\tau(t)\right]. \quad (4)$$

In Eq. (4) above the scaling factor $b(t)$ obeys the second-order differential equation

$$\ddot{b} + \omega^2(t)b = \omega_0^2/b^3 \quad (5)$$

with initial conditions $b(0) = 1$ and $\dot{b}(0) = 0$, the rescaled time parameter is determined by $\tau(t) = \int_0^t dt'/b^2(t')$, and $\phi_j(x, 0)$ are the well-known wave functions of the 1D harmonic oscillator with frequency ω_0 and eigenvalue E_j expressed in terms of the Hermite polynomials. We remark that Eq. (4) is the unique time-dependent solution of the linear Schrödinger equation (2).

Substituting the one-particle states (4) into Eq. (3) leads to the final result for the time evolution of the Tonks gas wave function in terms of its initial-time expression

$$\Phi_T(x_1, \ldots, x_N; t) = b^{-N/2}\Phi_T(x_1/b, \ldots, x_N/b; 0) \times \exp\left(\frac{i\dot{b}}{b\omega_0}\sum_j \frac{x_j^2}{2l_0^2}\right)\exp\left(-i\sum_j E_j\tau\right), \quad (6)$$

with $l_0 = \sqrt{\hbar/m\omega_0}$. Here we used that (i) the scaling (4) takes place irrespective of the one-particle quantum number, and (ii) the unit antisymmetric operator $\mathcal{A}$ is invariant under the scaling transformation.

Equation (6) allows an immediate derivation of an analytic expression for the one-body density matrix, given by its first-quantized expression $g_1(x, y; t) = N\int dx_2, \ldots, dx_N \Phi^*(x, x_2, \ldots, x_N; t)\Phi(y, x_2, \ldots, x_N; t)$, in the scaling form

$$g_1(x, y; t) = \frac{1}{b}g_1\left(\frac{x}{b}, \frac{y}{b}; 0\right)\exp\left(-\frac{i}{b}\frac{\dot{b}}{\omega_0}\frac{x^2 - y^2}{2l_0^2}\right). \quad (7)$$

This result shows first of all that during the generic time evolution described by Eq. (1) the absolute value of the one-body density matrix preserves its power-law behavior at large distances [9,22]. For the case of an expansion this was noticed in Ref. [18] from numerical simulations on a lattice. Secondly, Eq. (7) yields the exact evolution of the Tonks gas density profile $\rho(x; t) \equiv g_1(x, x; t) = \rho(x/b; 0)/b$, thus generalizing the result of Ref. [17] for any time evolution of the trap frequency. We remark that Eq. (7) also holds at any finite temperature, as follows from the statistical Bose-Fermi mapping theorem [23].

The dynamical phase in Eq. (7) enters the expression for the time evolution of the momentum distribution $n(p, t) = \int dxdy e^{ip(x-y)/\hbar}g_1(x, y; t)$, which upon change of integration variables x/b, $y/b \to x, y$ reads

$$n(p, t) = b\int dxdy g_1(x, y; 0) \times \exp\left[-ib\left(\frac{\dot{b}}{\omega_0}\frac{x^2 - y^2}{2l_0^2} - \frac{p(x - y)}{\hbar}\right)\right]. \quad (8)$$

Below we describe two cases where the dynamical phase acquired by the one-body density matrix strongly influences the time behavior of the momentum distribution.

Expansion.—A 1D expansion could be achieved in an experiment by turning off only the longitudinal confinement. To describe this case we set $\omega(t \leq 0) = \omega_0$ and $\omega(t) = 0$ for $t > 0$, and the solution of Eq. (5) for the scaling parameter $b(t)$ is given by $b(t) = \sqrt{1 + \omega_0^2 t^2}$. As this parameter becomes increasingly large with time, we are able to determine analytically the behavior of the momentum distribution (8) for long times by the method of stationary phase. The points for which the phase is stationary are given by $x^* = y^* = \omega_0 p l_0^2/(\dot{b}\hbar)$, and hence we find that the momentum distribution is asymptotically determined solely by the diagonal part of the equilibrium one-body density matrix, i.e., the particle density profile $\rho(x; 0)$ which is identical to the one of an ideal Fermi gas. For the case of harmonic confinement the latter is proportional to the equilibrium momentum distribution $n_F(p)$ of the ideal Fermi gas [24] thus allowing one to write the final expression for the Tonks gas momentum distribution as

$$n(p, t) = |\omega_0/\dot{b}| n_F(\omega_0 p/\dot{b}). \quad (9)$$

This result can be also understood as follows. Since the initial momentum distribution of the atoms is very narrow, the final momentum distribution is determined by the hydrodynamic velocity field acquired during expansion. Such a velocity field is obtained from the dynamical phase in the Eq. (7) and is linear in the position. Hence its distribution has the same shape as the particle density profile of a Fermi gas. For $N \gg 1$ Eq. (9) is well described by the Thomas-Fermi approximation, which neglects the quantum shell oscillations of order $1/N$ [25],

$$n(p, t) \simeq 2(l_0^2/\hbar)|\omega_0/\dot{b}|\sqrt{P_F^2 - (\omega_0 p/\dot{b})^2}. \qquad (10)$$

with $P_F = \hbar\sqrt{2N}/l_0$ being the Fermi momentum.

We estimate the characteristic time, t_F, for such "dynamical fermionization" by considering that in the Thomas-Fermi regime the one-body density matrix depends on coordinates only through the dimensionless ratios x/R and y/R. By rewriting Eq. (8) in such rescaled coordinates and in terms of p/P_F we see that the large parameter governing the dynamic phase in Eq. (8) is $Nb\dot{b}/\omega_0$, and thus we find $t_F \sim 1/N\omega_0 \sim \hbar/E_F$, E_F being the Fermi energy.

Equation (9) provides an accurate description of the momentum distribution for long times and for small momenta $p \leq P_F$. We proceed now to derive the second exact result regarding the large momentum behavior of $n(p, t)$ at all times. From the scaling solution (6) it follows that during its time evolution the many-body wave function displays the same type of cusp singularity as in its equilibrium configuration. Since no additional singularity is present in the dynamical phase, this cusp determines alone the large momentum behavior of the momentum distribution, as in the case of the equilibrium solution [10]. Hence, we find a power-law decay of the momentum distribution at large p, with an additional time-dependent suppression factor which originates from the dilatation of the interparticle distances during the expansion,

$$n(p, t) \sim p^{-4} b^{-3}. \qquad (11)$$

This complements the result (9) showing that at time $t \geq 1/\omega_0$ the fermionization of the momentum distribution is complete and the large-p tails are negligible.

We have tested the above predictions and explored the expansion at early times by numerically evaluating the momentum distribution Eq. (8) with a fast Fourier transform method using the explicit expression of the initial-time one-body density matrix in terms of a determinant of Hankel type [9]. The results, reported in Fig. 1, show that a broad Fermi distribution rapidly develops during expansion, followed by small adjustments of the quantum shell oscillations, while the p^{-4} tails become less and less important at long expansion times.

Oscillations.—As a second example, we consider now the case of an abrupt change of the trap frequency which induces large-amplitude "breathing" oscillations in the gas; i.e., we set $\omega(t \leq 0) = \omega_0$ and $\omega(t) = \omega_1$ for $t > 0$, with $\omega_1 < \omega_0$. The solution of Eq. (5) is

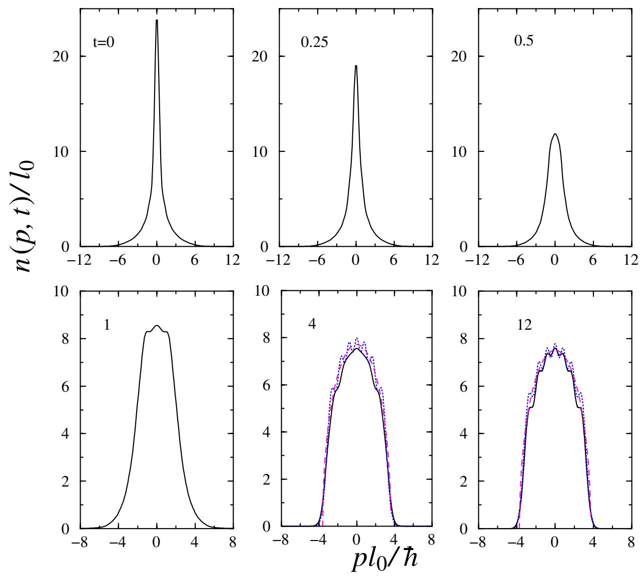

FIG. 1 (color online). Momentum distribution of an expanding Tonks gas with $N = 7$ at different times (in units of $1/\omega_0$) as indicated on the panels, from numerical solution (solid lines), asymptotic fermionic limit (dotted lines) and Thomas-Fermi approximation (dashed lines). The units are indicated on the axis labels.

$$b(t) = \sqrt{1 + (\omega_0^2 - \omega_1^2)\sin^2(\omega_1 t)/\omega_1^2} \qquad (12)$$

which describes periodic oscillations between one and ω_0/ω_1 with period $T = \pi/\omega_1$.

The dynamical evolution of the cloud in coordinate space is described, according to Eq. (7), by the self-similar breathing of the density profile with a time law given in Eq. (12). Notice that the solution (12) implies that the oscillation is undamped. The time evolution in momentum space, given by Eq. (8), displays a richer structure, and, in particular, an oscillating behavior between a bosoniclike and fermioniclike momentum distribution which is illustrated in Fig. 2. The main features of the dynamics may be understood by the following analytical considerations. When the condition $Nb\dot{b}/\omega_0 > 1$ holds, the stationary phase method can be employed, yielding that a time-dependent Fermi-like structure develops as in Eq. (9), and that the large-wavevector tails are suppressed as in Eq. (11). In the regime $N \gg 1$ and $\omega_0 \gg \omega_1$ this result is valid for most values of t, and closely resembles the dynamics of an ideal Fermi gas. The latter is given by the exact expression [26]

$$n(p, t) = B(t) n_F(B(t)p). \qquad (13)$$

with $B = b/\sqrt{1 + b^2\dot{b}^2/\omega_0^2}$ being related to the scaling of the kinetic energy [$B(t) = 1$ for the expansion]. In a small time interval $\omega_0 \Delta t = N^{-1}\omega_0^2/(\omega_0^2 - \omega_1^2)$ around the turning point $t = T/2$ the fermionic description does not hold. There, using Eq. (8) we find that the atomic cloud recovers

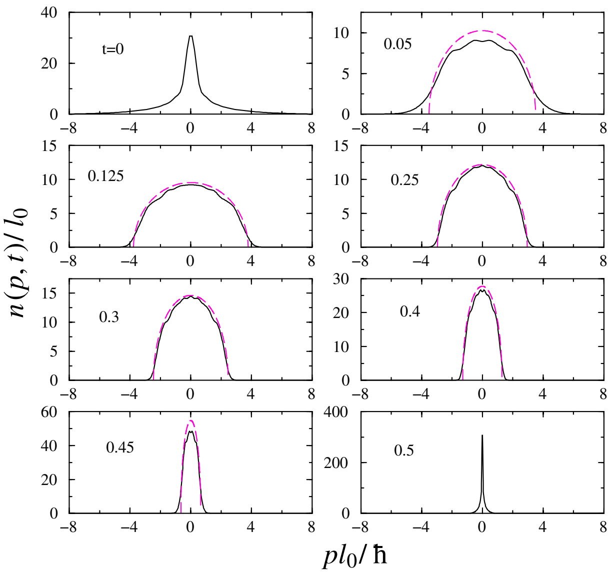

FIG. 2 (color online). Momentum distribution of an oscillating Tonks gas with $N = 9$ and $\omega_0/\omega_1 = 10$ at different times (in units of $T = \pi/\omega_1$) indicated on the panels, from numerical solution (solid lines) and Thomas-Fermi approximation (dashed lines). The units are indicated on the axis labels.

the initial bosonic momentum distribution rescaled by a factor $b_{\max} = \omega_0/\omega_1$, according to $n(p, T/2) = b_{\max} n(b_{\max} p, 0)$.

In conclusion, we have shown that the dynamical phase acquired by the many-body wave function during the evolution is responsible for the dynamical fermionization found in the 1D expansion and that during a large-amplitude breathing mode the cloud displays oscillations in momentum space between a Fermi-like and a Bose-like structure.

In this work we have considered only the Tonks-Girardeau limit of the Lieb-Liniger model. In this case the scaling transformation is exact and predicts a coherent, undamped motion of the cloud, which is a very peculiar feature of the Tonks regime. We suggest that the absence of damping in the breathing modes may be used to characterize the truly Tonks regime: for finite values of the coupling strength we expect instead a damped motion of the oscillations. Our predictions directly apply to the experiments on ultracold atomic gases in tight optical traps, where the time evolution of the momentum distribution should be experimentally accessible by allowing a 3D expansion of the cloud [13].

We thank E. Bogomolny, O. Bohigas, S. Brazovsky, L. P. Pitaevskii, and G. V. Shlyapnikov for valuable comments and discussions. We acknowledge support from the Centre National de la Recherche Scientifique (CNRS) and from the Ministère de la Recherche (Grant ACI Nanoscience 201). A. M. acknowledges financial support from SNS Pisa.

*LPTMS is a mixed research unit (UMR 8626) of CNRS and Université Paris-Sud.

[1] E. H. Lieb and W. Liniger, Phys. Rev. **130**, 1605 (1963); E. H. Lieb, Phys. Rev. **130**, 1616 (1963).
[2] D. S. Petrov, G. V. Shlyapnikov, and J. T. M. Walraven, Phys. Rev. Lett. **85**, 3745 (2000).
[3] M. Girardeau, J. Math. Phys. (N.Y.) **1**, 516 (1960); M. Girardeau, Phys. Rev. **139**, B500 (1965).
[4] V. Dunjko, V. Lorent, and M. Olshanii, Phys. Rev. Lett. **86**, 5413 (2001).
[5] P. Vignolo and A. Minguzzi, J. Phys. B **34**, 4653 (2001); C. Menotti and S. Stringari, Phys. Rev. A **66**, 043610 (2002).
[6] D. M. Gangardt and G. V. Shlyapnikov, Phys. Rev. Lett. **90**, 010401 (2003); D. M. Gangardt and G. V. Shlyapnikov, New J. Phys. **5**, 79 (2003).
[7] A. Lenard, J. Math. Phys. (N.Y.) **5**, 930 (1964); H. G. Vaidya and C. A. Tracy, Phys. Rev. Lett. **42**, 3 (1979); M. Jimbo, T. Miwa, Y. Mori, and M. Sato, Physica (Amsterdam) **1D**, 80 (1980).
[8] T. Papenbrock, Phys. Rev. A **67**, 041601(R) (2003).
[9] P. J. Forrester, N. E. Frankel, T. M. Garoni, and N. S. Witte, Phys. Rev. A **67**, 043607 (2003).
[10] A. Minguzzi, P. Vignolo, and M. P. Tosi, Phys. Lett. A **294**, 222 (2002); M. Olshanii and V. Dunjko, Phys. Rev. Lett. **91**, 090401 (2003).
[11] B. L. Tolra *et al.*, Phys. Rev. Lett. **92**, 190401 (2004).
[12] T. Stöferle *et al.*, Phys. Rev. Lett. **92**, 130403 (2004).
[13] B. Paredes *et al.*, Nature (London) **429**, 277 (2004).
[14] T. Kinoshita, T. Wenger, and D. S. Weiss, Science **305**, 1125 (2004).
[15] M. D. Girardeau and E. M. Wright, Phys. Rev. Lett. **84**, 5691 (2000).
[16] M. D. Girardeau and E. M. Wright, Phys. Rev. Lett. **84**, 5239 (2000).
[17] P. Ohberg and L. Santos, Phys. Rev. Lett. **89**, 240402 (2002).
[18] M. Rigol and A. Muramatsu, Phys. Rev. Lett. **94** 240403 (2005).
[19] V. S. Popov and A. M. Perelomov, Sov. Phys. JETP **30**, 910 (1970); A. M. Perelomov and Y. B. Zel'dovich, *Quantum Mechanics* (World Scientific, Singapore, 1998).
[20] Yu. Kagan, E. L. Surkov, and G. V. Shlyapnikov, Phys. Rev. A **54**, R1753 (1996).
[21] B. Sutherland, Phys. Rev. Lett. **80**, 3678 (1998).
[22] D. M. Gangardt, J. Phys. A **37**, 9335 (2004).
[23] K. K. Das, M. D. Girardeau, and E. M. Wright, Phys. Rev. Lett. **89**, 170404 (2002).
[24] During the expansion the momentum distribution of an ideal Fermi gas is stationary, see the discussion after Eq. (13).
[25] M. L. Mehta, *Random Matrices* (Academic Press, Boston MA, 1991), 2nd ed, Chap. 5, and references therein.
[26] This follows by applying the scaling transformation to the fermionic one-body density matrix, and using Eq. 7.374(8) of I. S. Gradshteyn and I. M. Ryzhik, *Tables of Integrals, Series and Products* (Academic Press, San Diego, 2000) to compute the Fourier transform.